Investigation of the Sensitivity of the Boundary Layer to DRE on Rotor Blade

Meng Wang[1,*], Hongjie Zhong[1], Ximing Yang[1], Ronghuan Zhao[1]

[1]Aero Science Key Lab of High Reynolds Aerodynamics Force at High Speed,
AVIC Aerodynamics Research Institute, Shenyang, 110034, China
*corresponding author: 15040393944@139.com

Abstract An experimental study was carried out to investigate the problem of roughness-induced boundary layer transition and thesensitivity of boundary layer to the dimensions of DRE (distributed roughness elements).Experiments were conducted in the rotor blade whirl tower at AVIC ARI. The chord length of rotor blade is C=60mm, and the rotor radius is R=800mm. The tests were at seven rotational speeds between 300 rpm and 600 rpm, leading to the tip speeds be between V_{tip}= 25 m/s and V_{tip}= 40 m/s. Both a single roughness element and a row of DRE were applied on the lower blade surface at X/C=0.2. The shape factor of DRE changed from d/k = 4.8 to d/k= 9.6, where d and k is diameter and height of the roughness element, respectively. We considered the distance between the DRE and the transition locations in different Reynolds numbers. Infrared thermography was employed to detect boundary layer transition on the rotor blade. A method based on the ratio of turbulent and laminar areas was used to estimate the downstream transition locations. The results showed an inverse relation between the transition length and the Reynolds number. The critical Reynolds number corresponding to DRE of different dimensions were determined by this relation.The boundary layer transition position is mainly affected by the height of DRE, for Re_X =16000~40000, the optimal height of DRE is k = 0.15 ~ 0.2 mm, the optimal shape factor is d/k = 6 ~ 8.
Keywords: boundary layer transition, DRE, infrared thermography, rotor blade

1 Introduction

Boundary layer transition has been a hot topic in the theory and engineering application research constantly. Scaled models are commonly used in the aerodynamic experimental research on the fixed wing aircraft or propeller, due to the scale effect, transition location on the test models is different from that on the full scale wing. In order to simulate the boundary layer flow condition of the test models, DRE (distributed roughness elements) are commonly used to fix boundary layer transition in experiments. The DRE should be large enough to trigger the transition while producing minimal drag. Hence, it is necessary to investigate the problems about roughness-induced boundary layer transition and the sensitivity of boundary layer to DRE.

The early investigations about the roughness-induced boundary layer transition were mainly accomplished by wind tunnel tests (Dryden (1953); Schubauer and Klebanoff (1955)).In the research on mechanism of boundary layer transition, Schubauer and Klebanoff (1955) measured the half-angle of the turbulent wedge induced by single cylindrical roughness element, and the detailed flow feature around the turbulent wedge was measured by using hot-wire anemometer.

Owing to the availability of large-scale computing resources, direct numerical simulation (DNS) on the laminar-turbulent transition was allowed in the last decade. Calculation of roughness-induced transition was performed in the low and high-speed regime (Rizzetta and Visbal (2007);Piot et al. (2008); Choudhary et al. (2010). DNS has the advantage of providing detailed information on the flow structure, but it requires large computational efforts, and individual studies can only cover a small portion of the large parameter space involved in roughness-induced transition (Bernardini et al. (2012)).

With the development of flow visualization measurement technology, a large number of non-intrusive measurement techniques for boundary layer transition have been put into application, including oil film interferometry (OFI), temperature sensitive paint (TSP), and infrared thermography (IRT). OFI was applied in wind tunnel experiments to full-scale tilt rotor blades (WadcicK et al. (1999)) and to high-speed model propeller blades (Schülein et al.(2012)). TSP was also applied on high-speed model propeller blades (Yorita et al. (2012)).

The IRT was first used in the 1960s and 1970s, particularly for reentry vehicles where high enthalpy flows provided enough signal for the relatively insensitive infrared cameras of the time (Schultz and Jones (1973)). With the improvement in sensitivity, IRT has been used extensively in convective heat transfer measurements in general (Astarita et al. (2000)) and wind tunnels particularly(De Luca et al. (1990)).Investigations of IRT for boundary layer transition measurement were carried out both in wind tunnel and in-flight experiments by Zuccher and Saric (2008),and Crawford et al. (2014). Crawford et al. (2014) proposed an automated technique for extracting quantitative transition location from raw IR images. IRT measurements on a rotating aerodynamic experiment were done by Mori et al. (2007). Raffel and Merz (2014) proposed differential infrared thermography (DIT) technique for the detection of unsteady boundary layer transition locations on a pitching airfoil and on rotating blade under cyclic pitch. Most recently, transition detection by high-speed infrared thermography was successfully demonstrated on model and full-scale helicopter rotors in hover condition (Richter and Schülein (2014); Raffel et al. (2015)). Contemporary infrared thermography has the advantage of high temperature resolution (~0.02 K), as compared to temperature-sensitive paint, which has a precision of ~0.1 K (Kowalewski et al. (2007)).

In this paper, an experimental study was carried out to explore roughness-induced boundary layer transition and the sensitivity of boundary layer to the dimensions of DRE. Both a single roughness element and a row of DRE were applied on the blade surface. Infrared thermography was employed to detect boundary layer transition on the rotor blade. A method based on the ratio of turbulent and laminar areas was used to estimate the downstream transition locations. The optimal dimensions of DRE were found by analyzing the relationship between transition length and Reynolds number.

2Transition detection by IRT

2.1 The principle of transition detection by IRT

IRT measures temperature distribution on the model surface by detecting the infrared radiation from the test model. The heat transfer characteristics can be obtained according to the temperature distribution on the model surface. Transition detection by IRT can be based on two heat transfer phenomenas associated with the change in the flow state from laminar to turbulent (Richter and Schülein (2014)).

For the flow with high Mach number and high temperature, the boundary layer recovery factor in turbulent flow is higher than that in laminar flow. The first approach is based on the increase in the boundary-layer recovery temperature in turbulent flow compared with laminar flow (Peake et al. (1977); Green, et al. (1983)). While, for the subsonic tests or at temperatures close to ambient, the measurable temperature difference becomes very small. The second approach relies on the increase in the heat transfer rate that occurs when the flow state changes from laminar to turbulent. The convective heat transfer coefficient is larger for turbulent boundary layer than for laminar boundary layer. If the temperature of the model is different from the temperature of the flow, the increase in heat transfer rate leads to a faster temperature change on the surface in the turbulent flow regime than in the laminar region. This enhances the temperature contrast between the two areas in the IR image. The temperature difference between the model and air flow can be produced by means of heating the model, heating resistors and halogen lamps are commonly used for heating the model (Crawford et al. (2014); Raffel et al. (2015)).

2.2 Experimental method

A layer of black paint was sprayed on the surface of the model in order to make sure the emissivity of the model surface be larger than 0.7. The thickness of black paint is less than 20μm. Therefore it can be assumed that the aerodynamic behavior was not altered by the paint.

In previous studies, there were three ways to generate the temperature difference between the model and airflow.
a)   Heat the model by using halogen lamps radioactively (Raffel et al. (2015));

b) Heat the model by using heating resistors inside the model (Crawford et al. (2013,2014));
c) Heat or cool the model before experiment, to provide initial temperature difference between the model and air flow (Zuccher and Saric (2008)).

In this paper, two halogen lamps were used to heat the rotor blades.

The normalized grayscale intensity of the IR image is used to represent the temperature. The pixel intensity I is referred to the intensity of pure white Imax, which means that I/Imax=0 represents a black pixel and I/Imax=1 a white one.

2.3 Identification of boundary layer transition position

Fig. 1 provides a typical IR image of rotor blade with DRE, it shows that the transition downstream DRE presents a zigzag pattern. In this case, it is inadvisable to regard the transition point of some profile as the transition position of the whole measurement area. So an appropriate identification criterion of transition downstream the DRE should be used.

The gray scale distribution curve on the right side of Fig. 1 is extracted from the three sections in the IR image, the section 1,2,3 is located under laminar flow, transitional flow and turbulent flow respectively. It shows that, when the flow is laminar or turbulent, the gray level distribution is smoother and steadier, and the amplitude of gray level varies slightly. When the flow is transitional, the gray level distribution presents a peak – valley pattern and the amplitude of gray level changes enormously. Therefore, the transition position could be identified according to the amplitude of the gray level of each section along the flow direction.
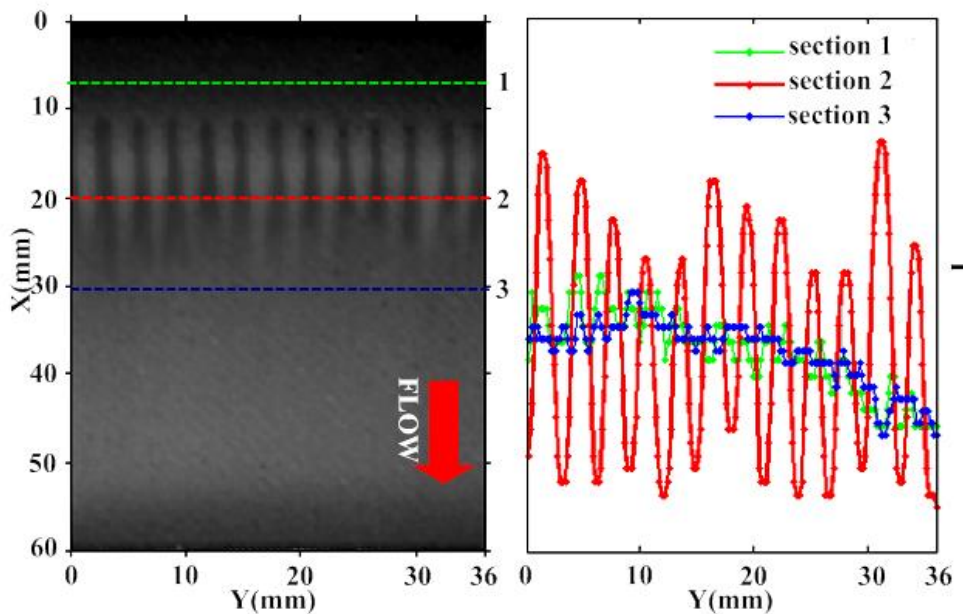
Fig. 1Typical transition pattern downstream the DRE

As shown in Fig. 2, an ideal boundary layer transition pattern downstream the DRE is presented. The points represent the roughness elements. And each triangle region represents the laminar flow between each two adjacent roughness elements, where the gray level is equal to 0. The area downstream the red regions represent turbulent flow, where the gray level is equal to 1. A periodic pulse curve represents gray level distribution that can be extracted from arbitrarily section in the direction of X. If the value of the pulse curve is 0, laminar is determined in the corresponding local region. The parameter i is used to represent the length of laminar within a period, m is the total length of a period. And w is defined as the ratio of the turbulent to total area, $w = 1 - i/m$, it indicates the development degree of transitional flow. When flow is fully laminar, w=0; when flow is fully turbulent, w=1. In this paper, the end of transition can be confirmed as long as

w>0.8.
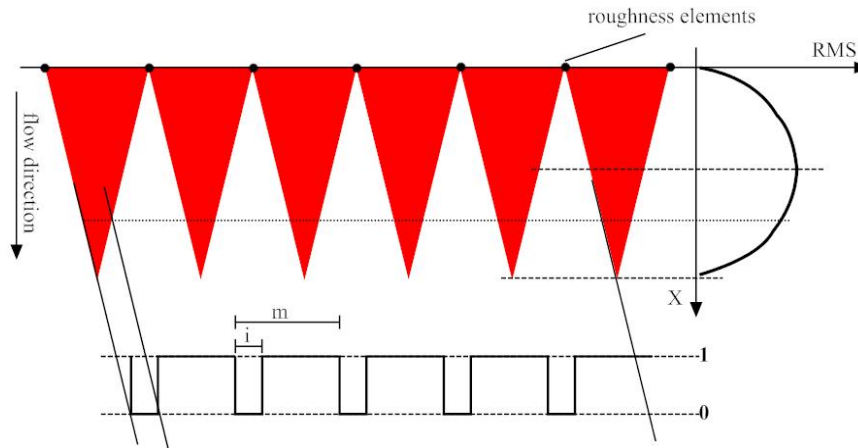
Fig. 2 Ideal boundary layer transition pattern downstream the DRE

The equation of the root mean square (*RMS*) of the gray level distribution of arbitrarily section in the direction of X is:

$$RMS = sqrt\left(\frac{i}{m} \cdot \left(1 - \frac{i}{m}\right)\right) = sqrt(w \cdot (1 - w)) \tag{1}$$

According to equation (1), the peak of the *RMS* curve appears at *w*=0.5, where *Rmax*=RMS (0.5)=0.5. *w*=0.8 is defined as a critical value, representing the end of the tradition. When *w*=0.8, we can obtain R_{80}=RMS(0.8)=0.4, R_{80}/*Rmax* =0.8, which means the transition position is the X coordinate corresponding to 80% of maximum *RMS*. In this case, the boundary layer transition position can be identified according to the *RMS* curve of IR image.

Fig. 3 illustrates the basic processes of the boundary layer transition identification. First of all, the *RMS* of the gray level of each section along direction X is calculated, and the curve of *RMS* versus X is obtained. The maximum *RMS* can be found. And then calculating R_{80} through the equation $R_{80} = 0.8 \times Rmax$. The X coordinate corresponding to R_{80} is the boundary layer transition position. The result is shown as a red dotted line in Fig. 3.
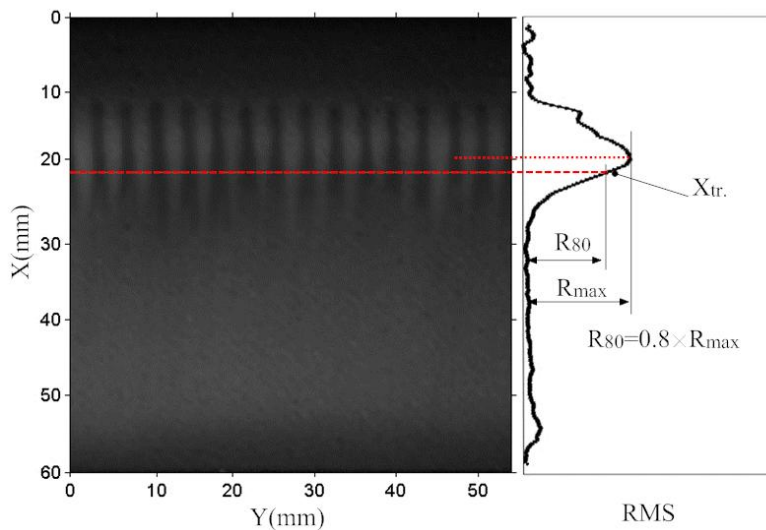
Fig. 3 Sketch of identification of boundary layer transition position

3 Experiment on a model rotor blade

3.1Experiment setup

Experiments were conducted in the rotor blade whirl tower at AVIC ARI. The test model was a rotor blade of model helicopter. The chord length of rotor blade is C=60mm, and the rotor radius is R=800mm. The measurement area is on the lower surface of the rotor blade. During the test, the angle of attack of rotating blade was 0.

As shown in Fig. 4, the experiment system consists of a rotor blade, two 350 W halogen lamps, photoelectric sensors and one IR camera. A FLIR SC7750L IR MCT-camera, sensitive in the 8.0-9.4μm wavelength range, was used. The resolution of IR image was 640× 512 pixels. The IR camera was placed under the lower surface of rotor blade, and the exposure time was designed to be IT=100μs to reduce image blurring. Using the photoelectric sensor to lock the phase of blade location, when the blade appeared in the IR camera FOV (field of view), trigger the IR camera to capture images. The rotor blade was radioactively heated by two 350 W halogen lamps to obtain a temperature difference of approximately 8 °C between the blade surface and the air flow. The air temperature was about 10 °C.
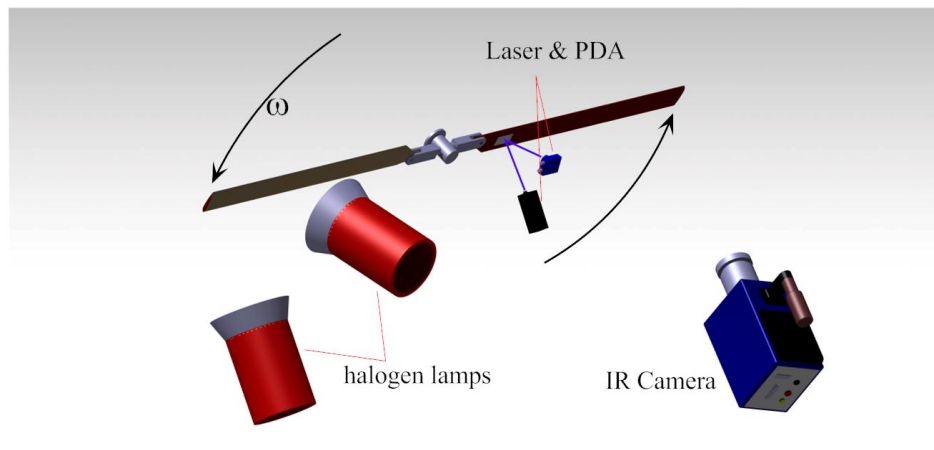
Fig. 4 Sketch of the experiment system

The cylindrical DRE were used in this paper. Three dimension parameters were utilized, as d and k were diameter and height of the roughness element respectively; l was the distance between two neighbor roughness elements.

The DRE was made of self-adhesive polyethylene. As shown in Fig. 5, a row of DRE were glued on the lower blade surface at X/C=0.2, r/R=0.9~0.98. The measurement area covers the tip region of rotor blade, r/R≈0.85-1.0.
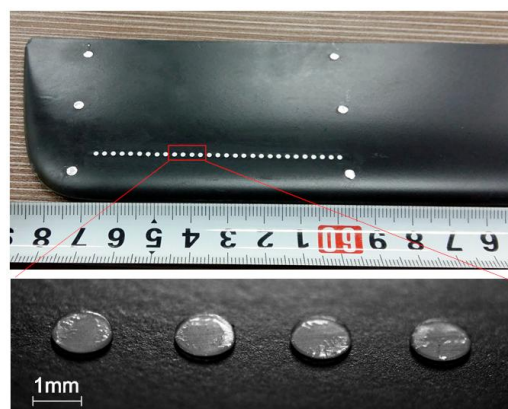
Fig. 5 The DRE used in current study, d=1.2, l=2.5, k=0.125 mm

3.2 Experimental scheme

The experiments were carried out according to the cases listed in table 1. The free transition experiments were conducted to provide basic conditions. A single roughness element (d=1.2, k=0.25mm) was applied on the blade surface at X/C=0.2, the rotor speed varied from 300 to 450 rpm. The angle of the turbulent wedge had been measured. The transition position downstream a row of DRE (d=1.2, k=0.25, l=3.6mm) had been estimated to verify the measurement results.

To analyze the relationship between boundary layer transition and dimension parameters of DRE, the DRE dimension parameters were defined: d = 1.2 mm, k = 0.125 ~ 0.25 mm, l = 2.5 ~ 3.6 mm.

Table 1 Experiment conditions

Size of DRE	Fixed transition location	Rotation speed	Velocity at r=750mm
k=0	Free transition	300~450 rpm	23.56~35.34 m/s
k=0.125, l=2.5mm	X/C=0.20	300~450 rpm	23.56~35.34 m/s
k=0.15 , l=2.5mm	X/C=0.25	300~600 rpm	23.56~47.12 m/s
k=0.20 , l=2.5mm	X/C=0.20	300~600 rpm	23.56~47.12 m/s
k=0.25 , l=2.5mm	X/C=0.20	300~450 rpm	23.56~35.34 m/s
k=0.25 , l=3.0mm	X/C=0.20	300~450 rpm	23.56~35.34 m/s
k=0.25 , l=3.6mm	X/C=0.20	300~450 rpm	23.56~35.34 m/s
(single element) k=0.25mm	X/C=0.20	300~450 rpm	23.56~35.34 m/s

4 Results and discussion

For the convenience of discussion, some parameters are defined firstly. V is the tangential velocity at r = 750 mm near the blade tip; C is the blade chord length; Xtr = X/C is the boundary layer transition position, Ltr is the transition length, which is equal to the distance between the actual transition position and DRE, for free transition condition, Ltr = Xtr × C.

The transition length Reynolds number $Re_{Ltr} = \rho \cdot V \cdot Ltr/\mu$, and the roughness element height Reynolds number $Re_k = \rho \cdot V \cdot k/\mu$.

4.1 Free transition

The free transition positions of each case were listed in table 2, the transition position was moving toward the leading edge of blade gradually as the flow speed V increases.

Table 2 The measurement results of free transition position

V(m/s)	Xtr (X/C)
23.56	0.8737
27.49	0.8436
31.42	0.824
35.34	0.8141

According to the result of free transition detection, the transition length Ltr and Re_{Ltr} were calculated. The Re_{Ltr} v.s. Re_C curve (Fig. 6) shows that, the transition length Reynolds number had a linear relation with chord length Reynolds number.
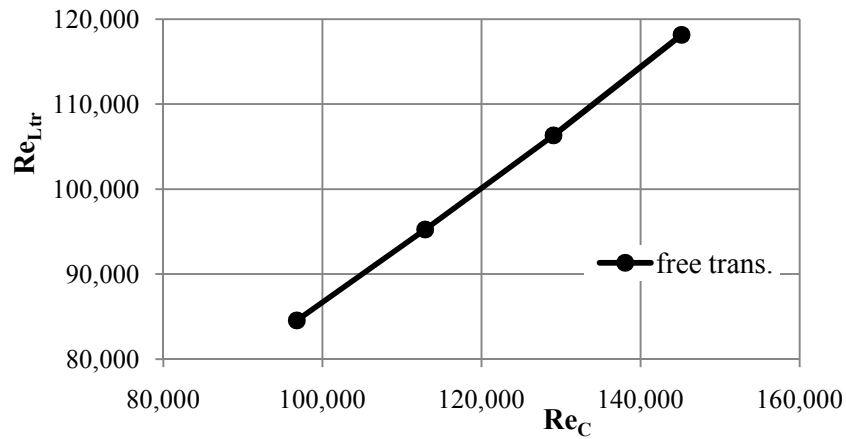
Fig. 6 The Re_{Ltr} v.s. Re_C curve.

4.2 Turbulent wedge and transition

If a particle of sufficient size is placed on the surface in a region of laminar flow, transition occurs at the particle, and a wedge-shaped region of turbulent flow extends downstream (Schubauer and Klebanoff (1955)).The angle of turbulent wedge induced by cylindrical roughness element had been observed in current study. The transition pattern downstream the DRE

Schubauer and Klebanoff (1955) studied the spreading mechanism of turbulent spots on the flat plate, and a 3.175mm cylindrical roughness element was applied on the flat plate 609.6 mm from leading edge. The flow speed was 24.38 m/s, the corresponding Re_X is about 84,800, measured half turbulence wedge angle was $\theta/2=6.4°\sim10.6°$, and hot-wire anemometer was used to understand the detailed flow structure in the transitional region.

In the current study, a single cylindrical roughness element (d = 1.2, k = 0.25 mm) was glued on the blade surface at X/C = 0.2, V = 23.56 ~ 35.34 m/s, the corresponding Reynolds number Re_X = 19,400 ~ 29,000. The IR images are shown in the Fig. 7, the canny operator was used to extract the edges in IR image at first; then the two straight lines of the turbulent wedge edge were detected by hough transform; finally, calculating the angle between the two straight lines, which is defined as the turbulent wedge angle θ, the measured results was θ = 6.13 ~ 9.98 °. θ increases as Re_X grows.
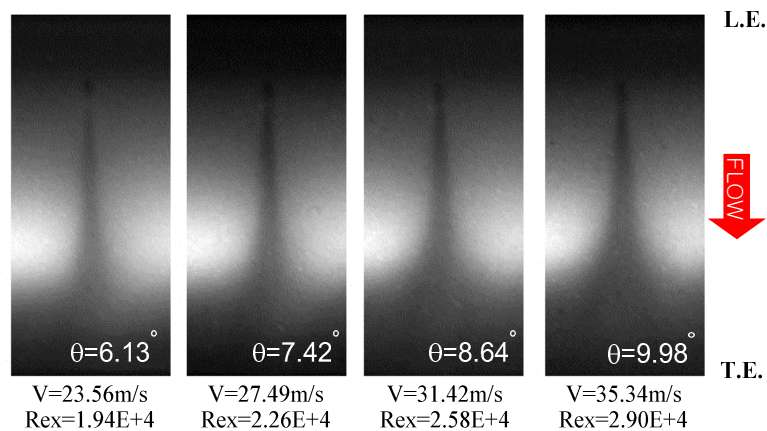
Fig. 7 The turbulent wedge induced by single roughness element, k=0.25mm, d=1.2mm

The transition length downstream DRE can be estimated according to the turbulent wedge angle. The estimated data and measurement data of transition length are compared in Fig.8, and it shows that the

measurement data are mainly consistent with the estimated data. So the measurement data are reliable, and this technique is suitable for the IR image of DRE patterns.
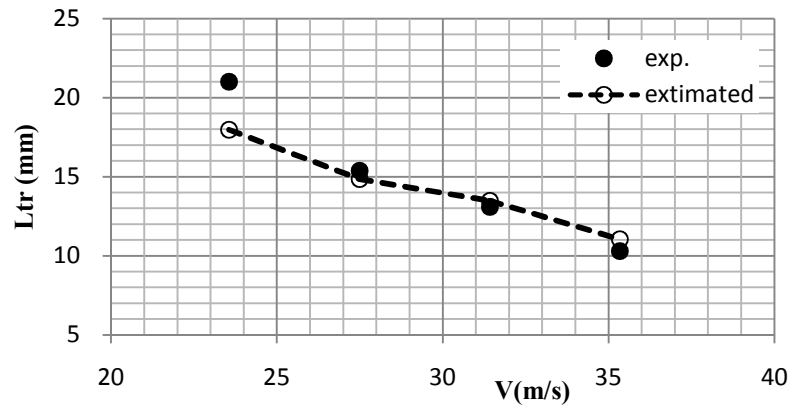
Fig. 8 Comparison of transition positions, DRE (d=1.2,k=0.25,l=3.6mm) fixed at X/C=0.2

4.3 Boundary layer transition induced by DRE

The boundary layer transition measurement results are listed in table 3. It shows that, the boundary layer transition position is moving towards the leading edge of blade with the flow speed and the height of DRE increasing. And the transition position is lightly affected by the distance between adjacent roughness elements. Relatively, the boundary layer transition position is mainly affected by the height of DRE.

Table 3 The transition measurement results.

V (m/s)	free trans.	DRE located ad x/C=0.2, l=2.5			l=3.0	l=3.6
		k=0.125	k=0.2	k=0.25	k=0.25	k=0.25
23.56	0.8737	0.7585	0.6545	0.5399	0.5492	0.5502
27.49	0.8436	0.7346	0.5409	0.4275	0.4535	0.4562
31.42	0.824	0.6953	0.4532	0.391	0.4096	0.4183
35.34	0.8141	0.6283	0.3858	0.3625	0.375	0.3717

The curves of transition length Reynolds number Re_{Ltr} of each dimension parameter of DRE are obtained from the experimental results (Fig. 9). For the condition of k = 0.125mm, when $Re_C<1.3\times10^5$, Re_{Ltr} increases as Re_C grows. Maybe the disturbance provided by DRE is not sufficient to trigger laminar transition to turbulent, the Re_{Ltr} curve maintain the trend like free transition condition (Fig. 6). When $Re_C>1.3\times10^5$, Re_{Ltr} begin to decrease. So the critical disturbance need for trigger laminar transition to turbulent is decrease as flow speed increasing.

For the condition of k = 0.15 and 0.2mm, there is a linearly inverse relation between Re_{Ltr} and the Re_C, and the slope of Re_{Ltr} curve for k = 0.2 is larger than that for k = 0.15mm. When k=0.25mm, there is a turning point on the Re_{Ltr} curve at $Re_C=1.1\times10^5$, and the Re_{Ltr} increase as the l grows.
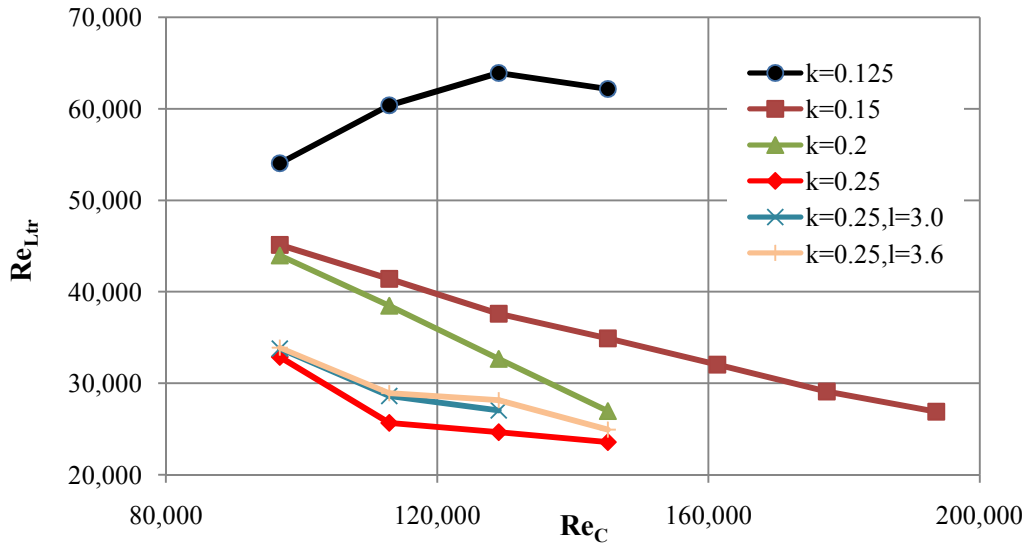
Fig.9 Re_{Ltr}v.s. Re_C curve

The relation between Re_{Ltr} and Re_k is shown in Fig. 10, the Re_{Ltr} decreases while Re_k increases. And the decrease rate of Re_{Ltr} increases gradually. The optimal Re_k is about 470~600, the corresponding height of DRE is h=0.15~0.25mm.
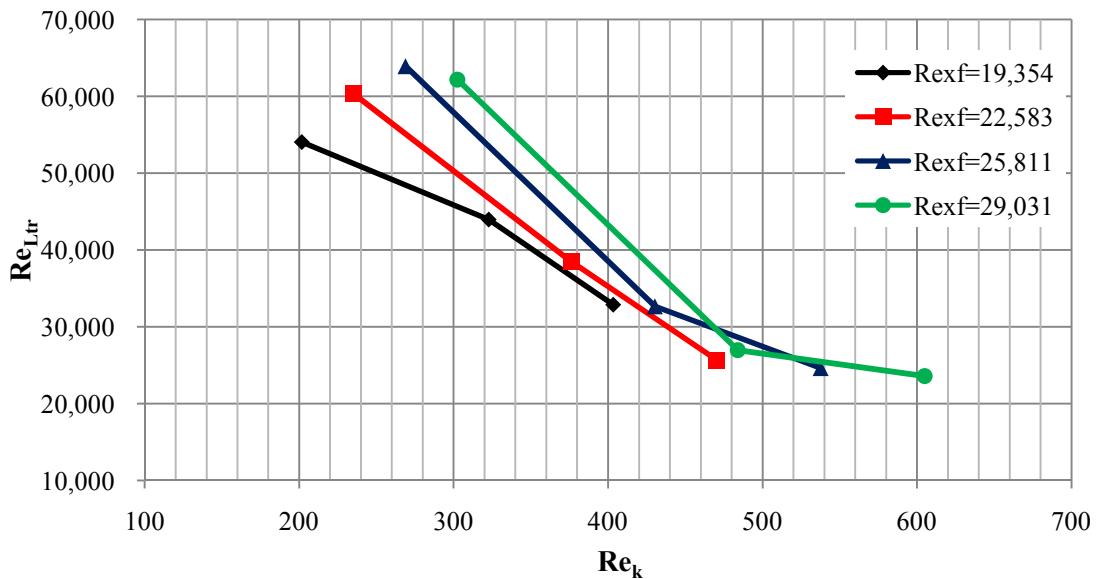
Fig. 10 Re_{Ltr} v.s. Re_h curve

Based on the analysis above, the transition location and the Reynolds number have an inverse relationship. The optimal dimension parameters of DRE for Re_X=16000~40000 are: k=0.15~0.2mm, l=2.5mm, d=1.2mm, the corresponding shape factor is d/k=6~8.

5Conclusion

The IRT technique was used to measure boundary layer transition on a rotor blade to study the problem of roughness-induced boundary layer transition and the sensitivity of boundary layer to the dimensions of DRE. Conclusions could be obtained:

a) The transition identification method based on laminar/turbulence zone area ratio is suitable for transition measurement downstream DRE. The calculation is convenient, and the result is stable and reliable;

b) For the cases of free transition, there is a linear relationship between the transition length Reynolds number Re_{Ltr} and chord length Reynolds number Re_C;

c) For Re_X = 19,400 ~ 29,000, the turbulent wedge angle produced by a single roughness element (d = 1.2, k = 0.25 mm) is θ = 6.13 ~ 9.98 °;

d) The boundary layer transition position is mainly affected by height of DRE, and as the increase in k, the transition position moves forward to the leading edge of blade. But, if k is too large, the efficiency of DRE to trigger transition will be reduced. For Re_X =16000~40000, the optimal height of DRE is k = 0.15 ~ 0.2 mm, the optimal shape factor is d/k = 6 ~ 8.

References

[1] Astarita T, Cardone G, Carlomagno GM, Meola C (2000) A surveyon infrared thermography for convective heat transfer measurements. *Optics and Laser Technology*, vol. 32(7–8), pp 593–610

[2] Astarita T, Carlomagno G M (2013) Applications. In: Smith J (ed) Infrared Thermography for Thermo-Fluid-Dynamics. Springer Heidelberg, New York Dordrecht London, pp 129-197, doi: 10.1007/978-3-642-29508-9

[3] Bernardini M, Pirozzoli S, Orlandi P (2012) Compressibility effects on roughness-induced boundary layer transition. *International Journal of Heat and Fluid Flow*, vol. 35, pp 45-51, doi:10.1016/j.ijheatfluidflow.2012.02.007

[4] ChoudharyM, LiF, Wu M, Chang C, EdwardsJ, Kegerise M, King R (2010).Laminar-turbulent transition behind discrete roughness elements in a high speed boundary layer. AIAA paper 2010-1575, 40th Fluid Dynamics Conferenceand Exhibit. Orlando, Florida

[5] Crawford B K, Duncan G T, West, D E, Saric W S (2013) Laminar-turbulent boundary layer transition imaging using IR thermography. *Optics and Photonics Journal*, vol. 3, pp 233-239, doi: 10.4236 /opj.2013.33038

[6] Crawford B K, Duncan G T, West, D E, Saric W S (2014) Quantitative boundary-layer transition measurements using IR thermography. In: Proceeding of the 52nd Aerospace Sciences Meeting, National Harbor, Maryland, AIAA 2014-1411, pp 1-10, doi: 10.2514/6.2014-1411

[7] Dryden H (1953) Review of published data on the effect of roughness on transition from laminar to turbulent flow. *Journal of Aeronautic Science*, vol. 20, pp 477–482

[8] De Luca L, Carlomagno GM, Buresti G (1990) Boundary layer diagnostics by means of an infrared scanning radiometer. *Experiments in Fluids*, vol. 9(3), pp 121–128

[9] Fey U, Egami Y, Engler R H (2006) High Reynolds number transition detection by means of temperature sensitive paint. 44th AIAA Aerospace Sciences Meeting and Exhibit, pp 1-19,doi: 10.2514/6.2006-514

[10] Green MJ, Budnik MP, Yang L, Chiasson MP (1983) Supporting flight-data analysis for space-shuttle orbiter experiments atNASA Ames Research Center. NASA TM-84345

[11] Kowalewski T, Ligrani P, Dreizler A, Schulz C, Fey U (2007) Temperature and heat flx. In: Tropea C, Yarin AL, Foss JF (eds) Handbook of experimental flid mechanics. Springer, Berlin, pp 488-553

[12] Mori M, Novac L, Sekavčnik M (2007) Measurements on rotating blades using IR thermography. *Exp. Thermal Fluid Sci.* 32(2), pp 387–396

[13] Peake DJ, Bowker AJ, Lockyear SJ, Ellis F (1977) Non-obtrusive detection of transition region using an infrared camera. AGARDCP-224

[14] Piot E, Casalis G, Rist U (2008) Stability of the laminar boundary layer flow encountering a rowof roughness elements: Biglobal stability approach and DNS. *European Journal of Mechanics B/Fluids*,

vol. 27, pp 684-706, doi: 10.1016/j.euromechflu.2008.01.007

[15] RizzettaD, Visbal M(2007)Direct numerical simulations of flow past an array ofdistributed roughness elements. *AIAA Journal*, vol. 45, pp 1967–1976

[16] RichterK, Schülein E (2014) Boundary-layer transition measurements on hovering helicopter rotors by infrared thermography. *Experiments inFluids* 55:1755, pp 1-13, doi: 10.1007/s00348-014-1755-z

[17] Raffel M, Merz C B (2014) Differential infrared thermography for unsteady boundary-layer transition measurements. *AIAA Journal*, vol.52(9), pp 2090–2093, doi: 10.2514/1.J053235

[18] Raffel M, Merz C B, Schwermer T, Richter K (2015) Differential infrared thermography for boundary layer transitiondetection on pitching rotor blade models. Experiments in Fluids 56:30, pp 1-30, doi: 10.1007/s00348-015-1905-y

[19] Schubauer G B,Klebanoff P S (1955)Contributions on the Mechanics of Boundary-Layer Transition. NACA-TN-3489, pp 853-863

[20] Schultz DL, Jones TV (1973) Heat transfer measurements in short-duration hypersonic facilities. AGAR Dograph 165, AGARD-NATO

[21] Sant Y L, Marchand M, Millan P, Fontaine J (2002) An overview of infrared thermography techniques used in large wind tunnels. *Aerospace Science and Technology*, vol. 6, pp 355-366

[22] Schülein E, Rosemann H, Schaber S (2012) Transition detectionand skin friction measurements on rotating propeller blades.28th AIAA aerodynamic measurement technology, ground testing and flght testing conference, NewOrleans, Louisiana, USA. Paper AIAA-2012-3202, doi:10.2514/6.2012-3202

[23] Wadcock AJ, Yamauchi GK, Driver DM (1999) Skin friction measurements on a hovering full-scale tilt rotor. *J Am Helicopter Soc*., 44(4), pp 312–319

[24] Yorita D, Asai K, Klein C, Henne U, Schaber S (2012) Transition detection on rotating propeller blades by means of temperature-sensitive paint. 50th AIAA Aerospace Sciences Meeting, Nashville, Tennessee, USA, Paper AIAA-2012-1187, doi:10.2514/6.2012-1187

[25] Zuccher S, Saric W S (2008) Infrared thermography investigations in transitional supersonic boundary layers. *Experiments in Fluids*, vol. 44, pp 145-157, doi: 10.1007/s00348-007-0384-1